

Electrocatalysis of chlorine evolution on different materials and its influence on the performance of an electrochemical reactor for indirect oxidation of pollutants

L. Szpyrkowicz^{a,*}, M. Radaelli^a, S. Daniele^b

^aDepartment of Environmental Sciences, University of Venice, Dorsoduro 2137, 30123 Venice, Italy

^bDepartment of Physical Chemistry, University of Venice, Dorsoduro 2137, 30123 Venice, Italy

Available online 20 January 2005

Abstract

Two different Ti/Pt–Ir materials (commercial and home made) and Ti/PdO + Co₃O₄ were investigated for their electrocatalytic properties versus Cl₂ evolution reaction. The materials were used in a batch electrochemical reactor to treat biologically recalcitrant di-azo compound. An electrochemically driven oxidation, mediated by a Cl₂/Cl[−] couple, proved efficient for destruction of this complex organic molecule, causing cleavage of the conjugated double bonds and destruction of unsaturated bonds. Both Ti/Pt–Ir materials performed well; lower kinetics obtained with the Ti/PdO + Co₃O₄ anode was caused by adsorption of the model compound, evidenced in preliminary voltammetric measurements. The dye oxidation reaction followed the second order kinetics with partial orders in the model compound and (time varying) chlorine concentrations equal to one. Specific energy consumption of 3.12 kWh m^{−3} proved the process more economic than the homogeneous phase oxidation.

© 2004 Elsevier B.V. All rights reserved.

Keywords: Electrocatalysis; Chlorine evolution; Indirect electro-oxidation; Electrochemical reactor; Anode material; Kinetics of indirect oxidation

1. Introduction

Sustainable industrial development is possible provided adequate measures to prevent emission of pollutants into the environment are undertaken. Among novel methods offering reduction of pollution, electrochemical technologies gain in popularity, due to their ability to destroy or modify pollutants without the recourse to additional chemicals. Chlorine-mediated electrooxidation is a particularly challenging tool for biologically recalcitrant contaminants that can be found in many industrial effluents [1,2]. In this process the anode material is fundamental, as electrochemical oxidation of Cl[−] ions to Cl₂ should proceed at a high rate. Moreover the anode should be inactive towards other species present in the electrolyte, in order to prevent active sites being blocked by adsorption. In this context it appeared pertinent to study the behaviour of some materials

with respect to generation of Cl₂ and to follow the performance of the electrochemical reactor for the removal of a model organic pollutant. The tested materials consisted of coatings composed of Pt + Ir and of Co + Pd, deposited on a Ti base. The choice of these coatings was performed considering that an addition of Ir (>20%) to Pt, which is a known catalytic material for Cl₂ evolution, prevents its passivation [3]. The Co + Pd coating was tested as the transition metal oxides [4] and Pd [5] are good electrocatalysts for the chlorine evolution reaction and, as such, potentially suitable for different applications of Cl₂ mediated electro-oxidation. Up to our knowledge a comparative study of the Cl₂ electrocatalysis on the materials considered in the present research has yet not been accomplished.

2. Experimental

Two different Ti/Pt–Ir anodes were subjected to investigation: a commercial one (indicated from now-on as Ti/Pt–Ir¹),

* Corresponding author. Tel.: +39 041 2348667; fax: +39 041 2348591.
E-mail address: lidia@unive.it (L. Szpyrkowicz).

produced by multiple paints-dry-furnace cycles, and a home-made (indicated as Ti/Pt–Ir²), obtained by a thermal method via brush painting (30 layers) of a water–methanol solution of H₂PtCl₆ and IrCl₄, intermediate (every second layer) drying at 350 °C and final drying at 530 °C. Both Ti/Pt–Ir electrodes had the same composition: 70% Pt and 30% Ir (molar percentage). A semi-quantitative X-ray analysis of the surface of the home-made electrode revealed the presence of a bi-metallic mixture of Pt and Ir, along with IrO₂ and PtO₂ (ca 30% (molar) quantities) and some trace quantities of TiO₂. The Ti/PdO–Co₃O₄ (termed later as Ti/Pd–Co) anode, consisting of Pd and Co oxides (proportion 70/30%, molar ratio) was prepared using: a CoCl₂ and PdCl₂ water–methanol solution, thermal decomposition at 280 °C (intermediate drying) and 430 °C final drying.

Preliminarily, voltammetric experiments were performed to establish the electrocatalytic activity of the studied materials towards Cl₂ evolution. The reaction investigated was:



which is the overall reaction of chlorine evolution. This reaction is a multi-step process, but under our conditions none of intermediate processes was studied in detail.

A classical three-electrode cell and Autolab PGSTAT20 potentiostat were used. Working electrodes were prepared by connecting pieces of the tested materials with a copper wire and sealing them in an epoxy resin. The counter electrode was a Pt spiral, while the reference electrode was an Ag/AgCl saturated with KCl. The base electrolyte solution was 0.1 M NaClO₄, adjusted with NaOH to pH 11.

Bulk electrolysis was performed in a batch reactor of 0.6 L working volume, equipped with a stainless steel cathode (10^{–2} m² area) and an anode (10^{–2} m² area) of the studied materials. The electrolysed solution was: 0.6 g L^{–1} of the model compound (a reactive dye Red Procion H-EXGL, Dystar, molecular structure shown in the insert of Fig. 1a), 16.25 g L^{–1} NaCl, 2.5 g L^{–1} Na₂CO₃ and 0.25 g L^{–1} NaOH. The reactor was under galvanostatic control and current density (c.d.) was varied from 200 to 800 A m^{–2}. The anode potential was measured against a home-made saturated calomel reference electrode (SCE), in a Luggin capillary probe, using a high impedance voltmeter (Keithley 169 Multimeter). The experiments were performed under isothermal condition at 40 °C ± 1, using a thermostatic bath (Haake DC30). Variation of the structure of the original dye molecule was evidenced by the loss of its colour, and the decrease of absorbance at 535 nm was chosen as the first figure of merit. Total organic carbon (TOC, Shimadzu 5050A Analyser) and pH were also monitored.

3. Results and discussion

3.1. Cyclic voltammetric investigation

Typical voltammograms recorded with Ti/Pd–Co and Ti/Pt–Ir electrodes in the base electrolyte, depicted in Fig. 1 a

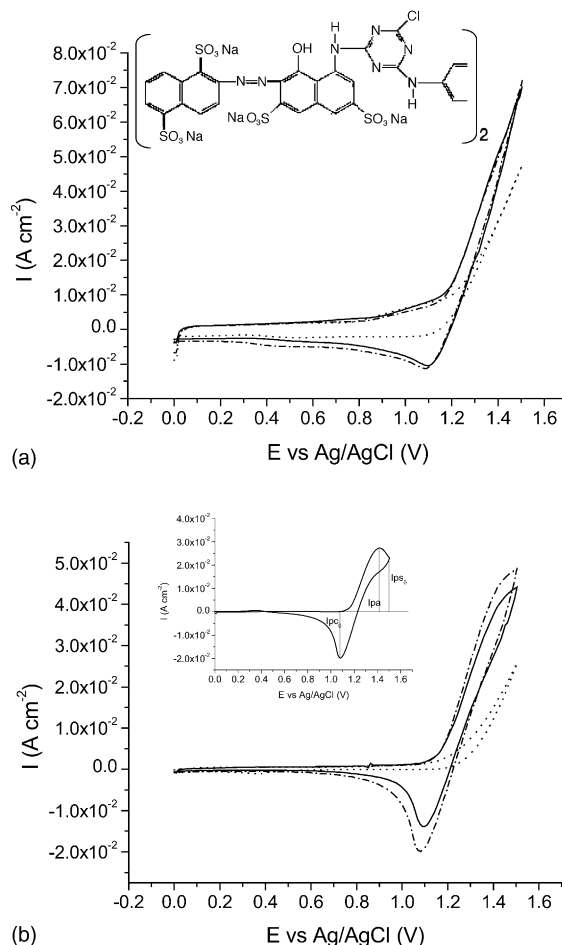


Fig. 1. Cyclic voltammograms (scan rate 0.05 V s^{–1}) recorded with: (a) Ti/Pt–Ir and (b) Ti/Pd–Co electrodes in an aqueous solution containing 0.1 M NaClO₄, pH 11, base electrolyte (dotted lines), 0.1 M NaCl (dash dot lines) and 0.15 g L^{–1} dye (solid lines); inset in: (a) molecular structure of the model compound, (b) cyclic voltammogram obtained after subtraction of the background current.

and b, show that over the positive potential region, the O₂ evolution process [6] rises at a potential > 1.2 V. This process is favoured at the Ti/Pt–Ir anodes, as indicated by 0.032 A cm^{–2} c.d. registred at 1.40 V, against 0.015 A cm^{–2} for the Ti/Pd–Co. After addition of NaCl to the base electrolyte an anodic wave, located at 1.40 ± 0.02 V, and an associated cathodic one at 1.09 ± 0.01 V, were observed on reversal of the potential scan. The anodic to cathodic wave separation was on average 0.31 ± 0.02 V, regardless of the electrode material and scan rates (ν) employed (over the range 5–100 mV/s). This anodic-cathodic system can be attributed to oxidation of Cl[–] ions to Cl₂ (overall reaction (1)). In fact, the height of the anodic wave depended almost linearly with concentration of Cl[–] ions, over the range 0.05–0.1 M.

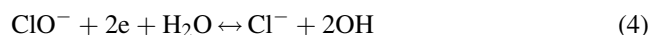
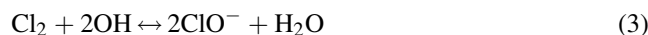
In order to verify whether the anodic and cathodic waves were under diffusion control, a series of cyclic voltammetric measurements at different (ν) were performed. The anodic (I_{pa}) and cathodic (I_{pc}) wave current and the cathodic to

anodic wave current ratio (I_{pa}/I_{pa}) were then examined against ν over the range 1–100 mV s⁻¹. Since the Cl⁻ oxidation occurred (cf. Fig. 1a and b) very close to the water discharge, a digital subtraction of the base electrolyte current was operated, providing cyclic voltammograms as that shown in the insert of Fig. 1b. Since the base line for the backward process cannot be determined from the voltammogram, the I_{pc}/I_{pa} ratio, and consequently I_{pc} , were evaluated [6] by equation (2). The meaning of I_{pc} and I_{ps_0} can be inferred from the insert of Fig. 1b.

$$\frac{I_{pc}}{I_{pa}} = \frac{I_{pc}}{I_{pa}} + \frac{0.45I_{ps_0}}{I_{pa}} + 0.086 \quad (2)$$

Both I_{pa} and I_{pc} depended linearly on $\nu^{1/2}$ ($r^2 > 0.99$) and I_{pc}/I_{pa} was equal to 0.99 ± 0.24 , irrespectively of the ν and electrode material, indicating that both the cathodic and anodic processes occurring at the studied materials are under diffusion control [6].

Under the alkaline pH, homogeneous reaction of Cl₂ disproportionation, generating ClO⁻ ions (reaction (3)), coupled to the heterogeneous electron transfer (reaction (1)), takes place. The reduction waves in Fig. 1 were found to be due to the reduction of ClO⁻ ions (reaction (4)):



Addition of the organic molecule to the electrolyte caused insignificant changes to the voltammetric features of the oxidation of Cl⁻ at the Ti/Pt–Ir electrodes (Fig. 1a). Small decrease of both anodic and cathodic wave currents was instead observed at the Ti/Pd–Co electrode (Fig. 1b). This can be ascribed to a slight passivation of the electrode surface due to adsorption.

3.2. Bulk electrolysis study

The rupture of the model organic compound, indicated by a complete decolourisation of the solution, was achieved under all the studied conditions, with the rates being a function of the anode material and c.d. Fig. 2(a)–(c) shows the performance of the reactor in terms of normalized absorbency (abs/abs₀). The spectra of the original dye solution and after electrochemical treatment are reported in the inset to Fig. 2a. The model dye solution shows an absorption band at $\lambda = 535$ nm, caused by the π – π^* transition of electrons in the azo group connecting disulfonated naphthalene group and naphthyl. Within the region near to ultraviolet ($\lambda = \text{ca } 280$ nm) its absorption band results from the unsaturated system of benzene and naphthalene rings. The UV after electro-oxidation reveals destruction of the conjugated azo-double bond and of unsaturated bonds; this latter effect seems to occur to a slightly lesser extend at the Ti/Pd–Co material, as can be deduced from a residual absorption at $\lambda \approx 280$ nm.

In Table 1 the main experimental details are reported along with the results expressed in terms of the kinetic rate

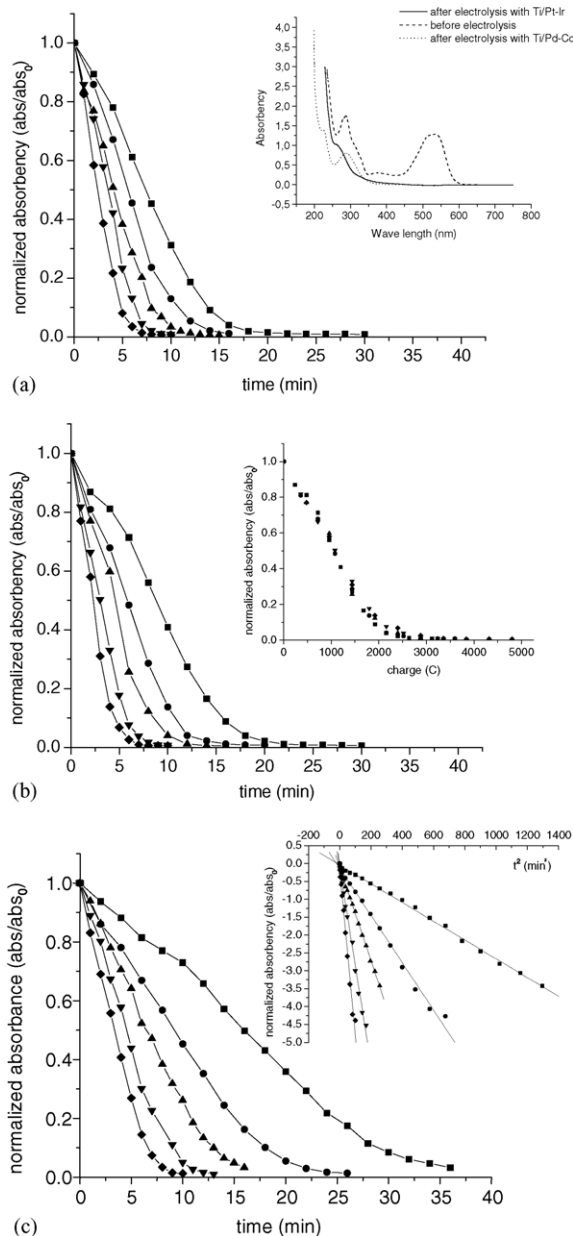


Fig. 2. Performance of the reactor during electrolysis of the model compound under various current densities: (■) 200, (●) 300, (▲) 400, (▼) 600 and (◇) 800 A m⁻² with: (a) Ti/Pt–Ir¹ anode; (b) Ti/Pt–Ir² anode; (c) Ti/Pd–Co anode; inset in: (a) UV–vis spectra of solutions before and after treatment; (b) time trends of the normalized absorbency vs charge for the Ti/Pt–Ir² anode and (c) plots of $k\Phi IA/2nFV$ vs. t^2 for the performance of the reactor equipped with the Ti/Pd–Co anode.

constants. The analysis of TOC revealed that no mineralisation occurred till the complete decolourisation was reached. A noticeable decrease of TOC was observable only after ca 8 kC of charge has passed.

Assuming a thickness of the reaction layer close to the diffusion layer [7] and equal to ca 10⁻⁵ m, the volume fraction of the reaction layer with respect to the total reactor volume would be ca 0.007%. Thus contribution of reactions occurring near the anode can be considered insignificant. It

Table 1
Experimental details and results

Parameter	Current density (A m^{-2})	Anode		
		Ti/Pt–Ir ⁽¹⁾	Ti/Pt–Ir ⁽²⁾	Ti/Pd–Co
Anode potential (V)	200	1.53	1.63	2.01
	300	1.64	1.79	2.16
	400	1.72	1.96	2.3
	600	1.92	2.28	2.56
	800	2.1	2.49	2.76
Cell potential (V)	200	4.04	4.14	4.52
	300	4.77	4.92	5.29
	400	5.53	5.77	6.11
	600	7.07	7.43	7.71
	800	8.47	8.86	9.13
Reaction rate constant $k \times 10^4 (\text{mol}^{-1} \text{m}^3 \text{s}^{-1})$	200	2.18 ($r^2 = 0.987$)	1.78 ($r^2 = 0.997$)	0.52 ($r^2 = 0.997$)
	300	2.38 ($r^2 = 0.987$)	2.34 ($r^2 = 0.979$)	0.91 ($r^2 = 0.996$)
	400	3.07 ($r^2 = 0.989$)	3.02 ($r^2 = 0.995$)	1.30 ($r^2 = 0.994$)
	600	3.66 ($r^2 = 0.993$)	3.99 ($r^2 = 0.989$)	1.80 ($r^2 = 0.992$)
	800	4.32 ($r^2 = 0.999$)	4.77 ($r^2 = 0.983$)	2.49 ($r^2 = 0.997$)
SEC (kWh m^{-3})	200	3.12	6.61	7.20
	300	4.33	4.47	7.94
	400	4.91	5.44	8.83
	600	7.54	7.05	11.95
	800	9.03	8.86	13.39

was assumed that decolourisation occurred essentially in the bulk solution via homogenous reactions, involving Cl_2 and chlorine-derived oxidants (termed “active chlorine”, “ Cl_2^* ”). As shown in Table 1 the anode potentials were higher than the normal potential for Cl_2 evolution ($E^\circ = 1.36 \text{ V}$), so this reaction was supposed to occur under all conditions of bulk electrolysis. The mass transport limited current density $I_L (\text{A m}^{-2})$ of Cl_2 evolution was estimated from: $I_L = nFk_m(\text{Cl}^-)$, where: n is the number of electrons ($n = 1$), F is the Faraday constant ($F = 96,500 \text{ C (mol e}^-)^{-1}$), k_m is the mass transport rate coefficient (m s^{-1}), (Cl^-) is the concentration of Cl^- ions in the solution (mol m^{-3}). The mass transport rate coefficient k_m determined by measuring the transport controlled oxidation of $0.01 \text{ M K}_4\text{Fe(CN)}_6$ was equal to $\text{ca } 2.2 \times 10^{-5} \text{ m s}^{-1}$. For $(\text{Cl}^-) = 278 \text{ mol m}^{-3}$, I_L for Cl_2 evolution was roughly estimated $I_L = 590 \text{ A m}^{-2}$. Even though, with an exception of 800 A m^{-2} , Cl_2 evolution can be hypothesised to be the main anode reaction, being the normal potentials of Cl_2 and O_2 evolution very close, the occurrence of this last reaction in parallel to Cl^- oxidation cannot be excluded.

In a solution containing “ Cl_2^* ” several radicals can be formed: ClO^\bullet , Cl^\bullet , OH^\bullet and H^\bullet [8], particularly in the presence of other oxidants, e.g. H_2O_2 . In the present study this compound could be formed by reduction [9], on the stainless still cathode containing Fe, of dissolved O_2 absorbed from the air. In fact, experiments conducted in a two-compartment cell (details not here presented) showed that decolourisation was three-fold faster in an undivided than in a two-compartment cell.

Differences in generation of Cl_2 with the tested electrocatalytic materials, evidenced during voltammetric investigation, were reflected by variation of the time trends

of elimination of colour during bulk electrolysis. While both the Ti/Pt–Ir anodes gave similar results despite their different origin, the Ti/Pd–Co electrode performed worse. Probably adsorption of the model compound could temporarily block some active sites making then unavailable for the Cl_2 evolution.

Trends of decolourisation were plotted in function of charge for all the anodes (an example for Ti/Pt–Ir shown in the inset of Fig. 2b). While for this material the experimental points overlap, suggesting that the same mechanism could be responsible for the destruction of the model compound at all c.d. applied, with the Ti/Pd–Co anode the performance was better the higher was the current. As shown in Table 1 to the increase of c.d. corresponded a rise of anode potentials, and it can be hypothesised that, at potentials higher than 2.16 V, higher oxides (+4) of Pd were formed (in analogy to other alervalent metallic cations containing anodes, e.g. the RuO_2 [10]) and could participate in oxidation of adsorbed organic molecules, via a mechanism involving OH^\bullet radicals, present at the surface [11].

Despite a first-order analytical model was supposed to well suit the purpose of evaluation of the reaction rate for here presented data, in analogy to electro-chlorination of naphthalene and other indirect electrochemical reactions [12], the destruction of the model compound followed the kinetics of the second order:

$$-\frac{d(\text{abs})}{dt} = k(\text{abs})C_{\text{Cl}_2} \quad (5)$$

where: k is the second order rate constant ($\text{mol}^{-1} \text{m}^{-3} \text{s}^{-1}$), abs is the measured absorbance, C_{Cl_2} is the concentration of “ Cl_2^* ” (mol m^{-3}). Concentration of “ Cl_2^* ” was a function of time and c.d. Assuming that the rates of Cl_2 loss reactions by

its cathodic reduction, its anodic oxidation to ClO_3^- and the quantity consumed in the homogeneous reaction with the dye were much lower than the production rate and thus can be considered insignificant, variation of Cl_2 concentration in time can be described by:

$$\frac{d\text{Cl}_2}{dt} = \frac{\Phi IA}{nFV} \quad (6)$$

where: I is the current density (A m^{-2}) and Φ - faradaic efficiency for chlorine evolution reaction. Integrating eq.(6) and substituting the expression for Cl_2 concentration in eq. (5) yields:

$$-\ln \frac{(\text{abs})_t}{(\text{abs})_0} = \frac{k\Phi IA}{2nFV} t^2 \quad (7)$$

The group $k\Phi IA/2nFV$ can be obtained from the slopes of the plots of $\ln(\text{abs}_t/\text{abs}_0)$ versus t^2 (an example shown in the inset to Fig. 2c). These values were used to calculate the second order rate constant k , taking current efficiency $\Phi = 0.85$, as indicated by our previous studies. The so obtained values are reported in Table 1. Lower k values obtained with Ti/Pd–Co anode than with the Ti/Pt–Ir materials, are congruent with the adsorption/passivation effect evidenced by voltammetric measurements. The values of k increase with the c.d., giving an indirect evidence of participation of other than " Cl_2 " oxidising species.

The highest kinetics of destruction of the dye molecule was obtained with the Ti/Pt–Ir⁽¹⁾ material, for which also the anode potential proved the lowest; thus this material, among the three anodes tested, seems to be the best electrocatalyst for the Cl_2 -mediated destruction of complex organic molecules. To evaluate the economics of the process, the specific energy consumption (SEC, kWh m^{-3}) was calculated from:

$$\text{SEC} = UIAt \quad (8)$$

where: U is the cell voltage (V), I is the c.d. (A m^{-2}), A is the surface area of the anode (m^2) and t is the time of electrolysis for a complete decolourisation (h). The values of SEC are reported in Table 1. Even though the rate of electrochemical destruction of the model compound increases linearly with c.d., a rise of the cell potential that accompanies this increase causes higher SEC for higher c.d. Thus 200 A m^{-2} is the optimal condition. The lowest value of $\text{SEC} = 3.12 \text{ kWh m}^{-3}$ corresponds to the cost of treatment of ca 0.3 € m^{-3} (taking the unit price of electric power equal to 0.1 € kWh^{-1}), as compared to 2.6 € m^{-3} , needed for the homogeneous phase reaction with hypochlorite (30 mL L^{-1} of a commercial hypochlorite solution were necessary to obtain a complete removal of colour; details not here presented).

4. Conclusions

Informations gained from voltammetric measurements indicated that all the three tested materials exhibit electrocatalytic properties towards Cl_2 evolution, and that this reaction, as well as the "active chlorine" loss reaction of hypochlorite reduction, proceeds at the studied anodes under diffusion control. The Ti/PdO– Co_3O_4 material can, however, be subjected to adsorption of organic compounds, that results in its partial passivation and a decrease of Cl_2 evolution. Experimental results showed that electrochemical oxidation mediated by the Cl_2/Cl^- couple is a feasible method to destroy complex organic molecules. The Cl_2/Cl^- redox mediator reacted with the model compound causing destruction of the conjugated azo-double bond and of unsaturated bonds. The reaction proved to follow the second order kinetic model, with partial orders in both the reagents equal to one. The reactor performed best when was equipped with the Ti/Pt–Ir material, for which no passivation was observed. Application of electrochemically mediated oxidation allowed the running costs to be reduced to ca 15% of the costs of oxidation with hypochlorite.

Acknowledgment

The authors wish to thank Magneto Chemie Special Anodes B.V, Netherlands, for providing the sample of Ti/Pt–Ir anodes.

References

- [1] L. Szpyrkowicz, C. Juzzolino, S. Daniele, M. De Faveri, Catal. Today 66 (2001) 519.
- [2] L. Szpyrkowicz, G.H. Kelsall, S.N. Kaul, M. De Faveri, Chem. Eng. Sci. 56 (2001) 1579.
- [3] G. Bianchi, J. Appl. Electrochem. 1 (1971) 231.
- [4] L.I. Krishtalik, Electrochim. Acta 26 (1981) 329.
- [5] K. Asami, K. Hashimoto, T. Masumoto, Electrochim. Acta 31 (1986) 481.
- [6] J. Bard, L.R. Faulkner, Electrochemical Methods, Wiley, New York, 1980.
- [7] Ch. Comninellis, A. Nerini, J. Appl. Electrochem. 25 (1995) 23.
- [8] I.G. Krasnobrodsko, Destruction Treatment of Wastewater from Dyes (in Russian ed.), Chimia, Leningrad, 1988, pp. 142–144.
- [9] E.J. Calvo, D.J. Schiffrin, J. Electroanal. Chem. 163 (1984) 257.
- [10] A. Harrison, D.L. Caldwell, R.E. White, Electrochim. Acta 28 (1983) 1561.
- [11] O. Simod, V. Schaller, C. Comninellis, Electrochim. Acta 42 (1997) 2009.
- [12] K. Scott, J. Electroanal. Chem. 248 (1988) 1.